Calibration and Analysis of the GCT Camera for the Cherenkov Telescope Array

Jason J. Watson

Brasenose College
University of Oxford

A thesis submitted for the degree of
Doctor of Philosophy

Trinity 2018

Abstract

Lorem ipsum dolor sit amet, consectetur adipiscing elit. Pellentesque sit amet nibh volutpat, scelerisque nibh a, vehicula neque. Integer placerat nulla massa, et vestibulum velit dignissim id. Ut eget nisi elementum, consectetur nibh in, condimentum velit. Quisque sodales dui ut tempus mattis. Duis malesuada arcu at ligula egestas egestas. Phasellus interdum odio at sapien fringilla scelerisque. Mauris sagittis eleifend sapien, sit amet laoreet felis mollis quis. Pellentesque dui ante, finibus eget blandit sit amet, tincidunt eu neque. Vivamus rutrum dapibus ligula, ut imperdiet lectus tincidunt ac. Pellentesque ac lorem sed diam egestas lobortis.

Suspendisse leo purus, efficitur mattis urna a, maximus molestie nisl. Aenean porta semper tortor a vestibulum. Suspendisse viverra facilisis lorem, non pretium erat lacinia a. Vestibulum tempus, quam vitae placerat porta, magna risus euismod purus, in viverra lorem dui at metus. Sed ac sollicitudin nunc. In maximus ipsum nunc, placerat maximus tortor gravida varius. Suspendisse pretium, lorem at porttitor rhoncus, nulla urna condimentum tortor, sed suscipit nisi metus ac risus.

Aenean sit amet enim quis lorem tristique commodo vitae ut lorem. Duis vel tincidunt lacus. Sed massa velit, lacinia sed posuere vitae, malesuada vel ante. Praesent a rhoncus leo. Etiam sed rutrum enim. Pellentesque lobortis elementum augue, at suscipit justo malesuada at. Lorem ipsum dolor sit amet, consectetur adipiscing elit. Praesent rhoncus convallis ex. Etiam commodo nunc ex, non consequat diam consectetur ut. Pellentesque vitae est nec enim interdum dapibus. Donec dapibus purus ipsum, eget tincidunt ex gravida eget. Donec luctus nisi eu fringilla mollis. Donec eget lobortis diam.

Suspendisse finibus placerat dolor. Etiam ornare elementum ex ut vehicula. Donec accumsan mattis erat. Quisque cursus fringilla diam, eget placerat neque bibendum eu. Ut faucibus dui vitae dolor porta, at elementum ipsum semper. Sed ultrices dui non arcu pellentesque placerat. Etiam posuere malesuada turpis, nec malesuada tellus malesuada.

Calibration and Analysis of the GCT Camera for the Cherenkov Telescope Array

Jason J. Watson

Brasenose College

University of Oxford

A thesis submitted for the degree of

Doctor of Philosophy

Trinity 2018

Acknowledgements

Personal

Lorem ipsum dolor sit amet, consectetur adipiscing elit. Vestibulum feugiat et est at accumsan. Praesent sed elit mattis, congue mi sed, porta ipsum. In non ullamcorper lacus. Quisque volutpat tempus ligula ac ultricies. Nam sed erat feugiat, elementum dolor sed, elementum neque. Aliquam eu iaculis est, a sollicitudin augue. Cras id lorem vel purus posuere tempor. Proin tincidunt, sapien non dictum aliquam, ex odio ornare mauris, ultrices viverra nisi magna in lacus. Fusce aliquet molestie massa, ut fringilla purus rutrum consectetur. Nam non nunc tincidunt, rutrum dui sit amet, ornare nunc. Donec cursus tortor vel odio molestie dignissim. Vivamus id mi erat. Duis porttitor diam tempor rutrum porttitor. Lorem ipsum dolor sit amet, consectetur adipiscing elit. Sed condimentum venenatis consectetur. Lorem ipsum dolor sit amet, consectetur adipiscing elit.

Aenean sit amet lectus nec tellus viverra ultrices vitae commodo nunc. Mauris at maximus arcu. Aliquam varius congue orci et ultrices. In non ipsum vel est scelerisque efficitur in at augue. Nullam rhoncus orci velit. Duis ultricies accumsan feugiat. Etiam consectetur ornare velit et eleifend.

Suspendisse sed enim lacinia, pharetra neque ac, ultricies urna. Phasellus sit amet cursus purus. Quisque non odio libero. Etiam iaculis odio a ex volutpat, eget pulvinar augue mollis. Mauris nibh lorem, mollis quis semper quis, consequat nec metus. Etiam dolor mi, cursus a ipsum aliquam, eleifend venenatis ipsum. Maecenas tempus, nibh eget scelerisque feugiat, leo nibh lobortis diam, id laoreet purus dolor eu mauris. Pellentesque habitant morbi tristique senectus et netus et malesuada fames ac turpis egestas. Nulla eget tortor eu arcu sagittis euismod fermentum id neque. In sit amet justo ligula. Donec rutrum ex a aliquet egestas.

Institutional

Lorem ipsum dolor sit amet, consectetur adipiscing elit. Ut luctus tempor ex at pretium. Sed varius, mauris at dapibus lobortis, elit purus tempor neque, facilisis sollicitudin felis nunc a urna. Morbi mattis ante non augue blandit pulvinar. Quisque nec euismod mauris. Nulla et tellus eu nibh auctor malesuada quis imperdiet quam. Sed eget tincidunt velit. Cras molestie sem ipsum, at faucibus quam mattis vel. Quisque vel placerat orci, id tempor urna. Vivamus mollis, neque in aliquam consequat, dui sem volutpat lorem, sit amet tempor ipsum felis eget ante. Integer lacinia nulla vitae felis vulputate, at tincidunt ligula maximus. Aenean

venenatis dolor ante, euismod ultrices nibh mollis ac. Ut malesuada aliquam urna, ac interdum magna malesuada posuere.

Abstract

Lorem ipsum dolor sit amet, consectetur adipiscing elit. Pellentesque sit amet nibh volutpat, scelerisque nibh a, vehicula neque. Integer placerat nulla massa, et vestibulum velit dignissim id. Ut eget nisi elementum, consectetur nibh in, condimentum velit. Quisque sodales dui ut tempus mattis. Duis malesuada arcu at ligula egestas egestas. Phasellus interdum odio at sapien fringilla scelerisque. Mauris sagittis eleifend sapien, sit amet laoreet felis mollis quis. Pellentesque dui ante, finibus eget blandit sit amet, tincidunt eu neque. Vivamus rutrum dapibus ligula, ut imperdiet lectus tincidunt ac. Pellentesque ac lorem sed diam egestas lobortis.

Suspendisse leo purus, efficitur mattis urna a, maximus molestie nisl. Aenean porta semper tortor a vestibulum. Suspendisse viverra facilisis lorem, non pretium erat lacinia a. Vestibulum tempus, quam vitae placerat porta, magna risus euismod purus, in viverra lorem dui at metus. Sed ac sollicitudin nunc. In maximus ipsum nunc, placerat maximus tortor gravida varius. Suspendisse pretium, lorem at porttitor rhoncus, nulla urna condimentum tortor, sed suscipit nisi metus ac risus.

Aenean sit amet enim quis lorem tristique commodo vitae ut lorem. Duis vel tincidunt lacus. Sed massa velit, lacinia sed posuere vitae, malesuada vel ante. Praesent a rhoncus leo. Etiam sed rutrum enim. Pellentesque lobortis elementum augue, at suscipit justo malesuada at. Lorem ipsum dolor sit amet, consectetur adipiscing elit. Praesent rhoncus convallis ex. Etiam commodo nunc ex, non consequat diam consectetur ut. Pellentesque vitae est nec enim interdum dapibus. Donec dapibus purus ipsum, eget tincidunt ex gravida eget. Donec luctus nisi eu fringilla mollis. Donec eget lobortis diam.

Suspendisse finibus placerat dolor. Etiam ornare elementum ex ut vehicula. Donec accumsan mattis erat. Quisque cursus fringilla diam, eget placerat neque bibendum eu. Ut faucibus dui vitae dolor porta, at elementum ipsum semper. Sed ultrices dui non arcu pellentesque placerat. Etiam posuere malesuada turpis, nec malesuada tellus malesuada.

Contents

List of Figures **vii**

Abbreviations **viii**

1 Introduction **1**
1.1 Plan 2
1.1.1 Topics 2
1.1.2 Questions 2

2 Camera Design & Mechanics **3**
2.1 Plan 3
2.1.1 Topics 3
2.1.2 Questions 3
2.2 Introduction 3

3 CTA Architecture **5**
3.1 Plan 5
3.1.1 Topics 5
3.1.2 Questions 5

4 Software **6**
4.1 Plan 6
4.1.1 Topics 6
4.1.2 Questions 6

5 Calibration **7**
5.1 Plan 8
5.1.1 Topics 8
5.1.2 Questions 8
5.2 Introduction 8
5.3 TARGET Calibration 9
5.3.1 Electronic Pedestal Subtraction 9
5.3.2 Transfer Function 11
5.4 Photosensor Calibration 14
5.4.1 CHEC-M 14
5.4.2 CHEC-S 15

5.5 Other 17
5.5.1 Timing Corrections 17
5.5.2 Temperature Corrections 18
5.5.3 LED Flashers 18
5.6 Future 19

6 Pipeline Reduction **20**
6.1 Plan 20
6.1.1 Topics 20
6.1.2 Questions 20

7 Camera Performance **21**
7.1 Plan 21
7.1.1 Topics 21
7.1.2 Questions 21

8 On-Sky Pipeline **22**
8.1 Plan 22
8.1.1 Topics 22
8.1.2 Questions 22

9 Summary **23**

References **24**

List of Figures

2.1 Functional block diagram of the TARGET 5 ASIC. 4

5.1 Spread of sample values from the residual waveforms resulting from applying the waveforms to the data used to produce them. 10

5.2 Same as 5.1, but split into increments of 10,000 events. 11

Abbreviations

AC Alternating Current.

ADC Analogue-to-Digital Converter.

ASIC Application-Specific Integrated Circuit.

CHEC Compact High Energy Camera.

CHEC-M Compact High Energy Camera (CHEC) using Multi-Anode Photomultiplier Tubes (MAPMTs) as the detector.

CHEC-S CHEC using Silicon Photomultiplier Tubes (SiPMTs) as the detector.

CTA Cherenkov Telescope Array.

DC Direct Current.

FEE Front-End Electronics.

FITS Flexible Image Transport System.

HV High Voltage.

IACT Imaging Atmospheric Cherenkov Telescope.

MAPMT Multi-Anode Photomultiplier Tube.

p.e. Photo-Electrons.

PDE Photon Detection Efficiency.

RMSE Root-Mean-Square Error.

SiPMT Silicon Photomultiplier Tube.

SPE Single Photo-Electron.

TARGET TeV Array Readout with GSa/s sampling and Event Trigger.

TARGET 5 TARGET (TeV Array Readout with GSa/s sampling and Event Trigger) (version 5).

TARGET C TARGET (version C).

Vped Pedestal voltage input into the TARGET ASIC.

1 Introduction

:

1.1 Plan

1.1.1 Topics

- High Energy Astrophysics
  - Fermi
  - Fermi Bubbles
  - HAWC
- IACTs
- CTA
- CTA Science
  - Science Cases
  - Use "Science with CTA" paper
- SSTs
- SST Science
  - What do we contribute?
  - What can't be done without us?
- GCT
- CHEC
  - What makes us better?
  - Advantages of Schwarzchild-Couder
    - Increased FoV
    - Size
    - Cost
  - Advantages of full waveform readout
  - Other Advantages?
    - Trigger
    - Energy/power/voltage Requirements
    - Commonalities (SCT)

1.1.2 Questions

- ?

2

Camera Design & Mechanics

Contents

1.1 Plan **2**
1.1.1 Topics 2
1.1.2 Questions 2

:

2.1 Plan

2.1.1 Topics

- Introduce TARGET architecture & Wilkinson ADC
- Different TARGET versions
- FEE
- MAPMs
- SiPMS
  - How they work
  - Comparison investigations
  - Property trade-offs
- CHEC-M
- Changes for CHEC-S
- Future - MUSIC ASICs

2.1.2 Questions

- ?

2.2 Introduction

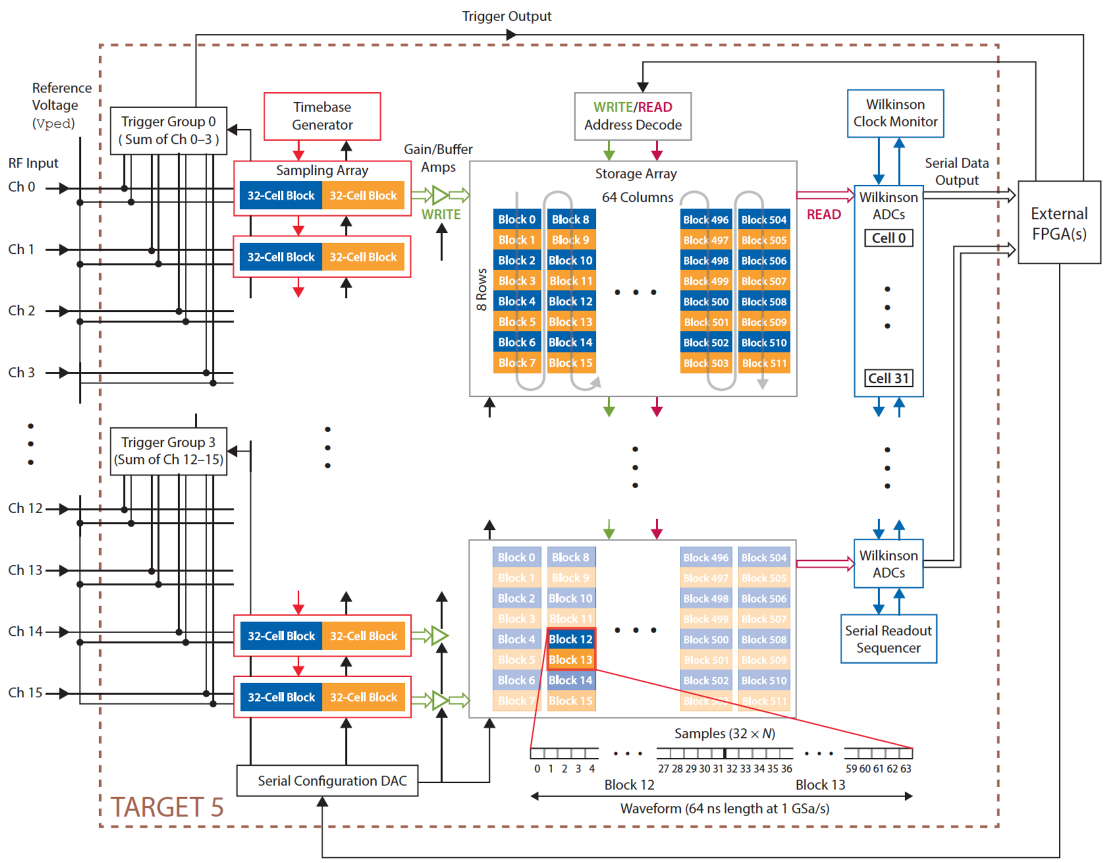

Figure 2.1: Functional block diagram of the TARGET 5 ASIC [1]

Add more details

3

CTA Architecture

Contents

2.1 Plan **3**
2.1.1 Topics 3
2.1.2 Questions 3
2.2 Introduction **3**

:

3.1 Plan

3.1.1 Topics

- Requirements
- Data Levels

3.1.2 Questions

- ?

4
Software

Contents

3.1 Plan **5**
3.1.1 Topics 5
3.1.2 Questions 5

:

4.1 Plan

4.1.1 Topics

- TargetIO/TargetDriver
- TargetCalib
- ctapipe
- gammapy/CTOOLS

4.1.2 Questions

- ?

5
Calibration

Contents

4.1 Plan 6
4.1.1 Topics 6
4.1.2 Questions 6

:

5.1 Plan

5.1.1 Topics

- Pedestal subtraction
- Transfer functions
- Gain Matching
- SPE
- Flat fielding
- Time correction
- Future
  - Live calibration

5.1.2 Questions

- TARGET architecture diagram, Wilkinson ADC
- How much detail about all the TF approaches do I go into?

5.2 Introduction

In order to obtain meaningful and reliable results from the camera, a number of calibrations must be applied to the waveforms read. A primary objective of my DPhil is to investigate the most optimal and efficient approaches for these calibrations (in accordance with the Cherenkov Telescope Array (CTA) requirements described in Chapter 3), and to determine if additional calibrations are required.

The calibrations applied have evolved during the course of the prototyping of CHEC; the calibrations applied to CHEC using MAPMTs as the detector (CHEC-M) waveforms are not the same for CHEC using SiPMTs as the detector (CHEC-S). Additionally, the calibration applied for the on-sky pipeline can differ slightly to the calibration used to obtain results such as the charge resolution.

When I joined the CHEC development, the calibration discussion was still in it's infancy. Some approaches had been tested in a laboratory environment [2], but there had been little discussion on how exactly the calibrations will be applied efficiently in an analysis pipeline, where one may not be able to use the same detailed calibration due to limited resources (such as memory and time). A major contribution of my DPhil was to prototype the calibrations procedures, develop an approach for a calibration pipeline, write the software to perform such a pipeline, and finally assess the performance of the pipeline. This was an iterative procedure, the development of which is still ongoing, however a procedure now exists that allows us to obtain meaningful results from the waveform data, a capability that is of paramount importance in the commissioning of the camera.

In this chapter I will outline the each of the calibration steps that are presently adopted for CHEC camera. They are introduced in the general order that they are applied, and split into the categories of TARGET ASIC (Application-Specific Integrated Circuit), photosensor, and "other" calibrations.

5.3 TARGET Calibration

The calibrations described in this section relate to the TARGET module. As detailed in Chapter 2, the TARGET ASIC is responsible for the sampling, digitisation and readout of the waveform data. As a result there are two calibrations that are solely related to the TARGET ASIC: electronic pedestal subtraction and the linearity correction via the transfer function.

The functional block diagram of the TARGET ASIC in Figure 2.1 outlines the electronics responsible for the need of these calibrations, and should be used as a reference in the following descriptions.

As the calibrations in this section are very low-level, and related to CHEC's specific Front-End Electronics (FEE), they are handled by the TargetCalib library (described in Chapter 4).

5.3.1 Electronic Pedestal Subtraction

The most important, but also the simplest calibration to apply is the subtraction of the electronic pedestal. Each of the cells in the storage array of the ASIC is a unique capacitor. For a specific input input pedestal voltage (Vped), each capacitor has its own resulting electronic pedestal value. As each sample of the waveform corresponds to a single storage cell, each sample therefore has a unique pedestal value to be subtracted. This is apparent in Figure where the variation from sample-to-sample is very large. This variation is large enough that low amplitude pulses are undetectable in the waveform (Figure)) and therefore it is paramount to subtract this per-sample pedestal.

Create figure showing the raw waveform and its pedestal subtracted form (no HV)

Figure with low amplitude pulse before and after pedestal subtraction, and high amplitude pulse the same, also mirrored camera image?

There are $2^{14} = 16,384$ storage cells per channel (for CHEC-M, $2^{12} = 4096$ for CHEC-S), therefore there are $32(Modules) * 64(Channels) * 16,384(Cells)$ pedestal values to keep record of. However, there is an additional contribution to the behaviour of the pedestal - discharging a cell to readout its value will slightly discharge adjacent cells. The result of this effect is that the further along in the waveform a cell is, the lower its pedestal value will be. An extra dimension of "position in waveform" consequently needs to be considered. This effect is illustrated in Figure , and its affect demonstrated in Figure .

Make sure to mention about the difference in number of cells for checs in ch2

include figures

Generation

In order to perform the pedestal subtraction, one must first generate the lookup table of pedestal values. This can be easily obtained with a calibration run where the photosensors are disabled by turning off the High Voltage (HV) , and forcing the camera to trigger (with either an external pulse generator, or internally via software) to obtain a large amount of waveform data. Typically around 30,000 events provide enough samples for every storage cell, in every waveform position, to be hit at least 10 times. The samples are then collected as a running average with the dimensions $[Module, Channel, StartingBlock, Blockphase + Sample\_i]$, where the $StartingBlock$ is the storage block that the first sample in the waveform belongs to (see Figure), $Blockphase$ is the cell index within the storage block that the waveform begins on, and $Sample\_i$ is the index of each sample in the waveform. This is illustrated in Figure , where for these two readout windows shown, the pedestal running average `Pedestal[TM][CHANNEL][9][8:103]` and `Pedestal[TM][CHANNEL][8][12:107]` will be contributed to respectively.

is it HV when considering the sipms?

include figure, and edit to use bp 8 and 12

Figure shows a visual representation of the pedestal lookup table for a single channel.

A figure showing the lookup table of the pedestal, for checm due to the storage block ordering. Annotate a single repeated

Figure 5.1

Insert and update

Figure 5.2

Insert and update, Also include extra plot versus event

The TargetCalib library handles this generation, and stores the pedestal look-up table into a FITS (Flexible Image Transport System). A new pedestal file is typically generated at the start of each new dataset, as its dependencies on temperature and evolution with time are still being investigated.

Application

To apply the pedestal, the entry within the lookup table that corresponds to each sample is subtracted from the waveform. The result of the calibration can be seen in Figures .

include figures from before

Performance

One quantification of this calibration's performance is the standard deviation per sample of the residual waveform from applying the pedestal subtraction to the data used to produce it. Figure 5.1 shows the spread in these values .

quote conversion into photo-electrons, and write actual resulting performance, and talk about if its good enough

This quantity informs about the intrinsic spread of the pedestal values about their mean, and can also indicate at some changes in pedestal value with time. Figure 5.2 demonstrates an occurrence of the pedestal value changing with time, and is investigated further in Section 5.5.2.

5.3.2 Transfer Function

The other calibration related to the digitisation and readout inside the TARGET ASIC is caused by the non-linearities in the storing and reading of charge to and from the storage cells. The components responsible for the need for this calibration are the sampling array, gain/buffer amps, and the Wilkinson Analogue-to-Digital Converters (ADCs), seen in Figure 2.1. As a result of the non-linearity of these components, the sample value readout does not scale linearly - a sample with twice the amplitude input into TARGET will have less than twice the amplitude when readout.

To correct for this non-linearity, a look-up table is generated to convert from the sample amplitude read-out (in ADC counts), to the input sample amplitude (in mV). This look-up table is known as the Transfer Function. As one might expect, each sampling cell has its own linear response to correct for, and therefore a look-up table is typically required at-least per channel and per sampling cell, however a noticeably improved performance is observed by considering a Transfer Function per storage cell . need to show this, maybe in TF Investigations appendix?

There are two forms of Transfer Function that have been considered for CHEC, distinguished by the type of input used to generate them. A Direct Current (DC) Transfer Function is created by applying a constant DC input of known voltage into the module, and iterating over the full dynamic range by varying the voltage. An Alternating Current (AC) Transfer Function is generated by inputting an AC signal (such as a pulse with the expected shape from the photosensor plus shaper) of known amplitude, and iterating as with the DC approach. During previous investigations of the TARGET module, where sinusoidal signals were input into the module, a dependence on the signal frequency and input amplitude was observed that acts to further reduce the output amplitude [2][1]. The source of this dependence was deemed to be due to the amplifiers, which cannot slew fast enough to keep up with the input signal if the frequency and amplitude are large.

Generation (DC Transfer Function)

During the commissioning of CHEC-M, a DC Transfer Function was used with no AC corrections. To generate this Transfer Function the internal input pedestal voltage (Vped) setting is used to apply a DC voltage offset of known amplitude. The full dynamic range of the module is explored by repeating the process for amplitudes between . quote the range The waveforms produced by these runs are read-out, and the running average is grouped and monitored according to $[Module, Channel, SamplingCell, InputAmplitude]$, utilising every sample in the waveform. Around 1,000 events are required to provide sufficient statistics. This produces a lookup table like the one shown in Figure . insert figure

The second step in the generation is to flip the axes of this lookup table, and linearly interpolate at the ADC points defined by the user. This provides a second lookup table that can be more efficiently used to provide a calibrated mV value for the measured ADC value (Figure). add figure This table is saved to a FITS file, ready for application.

Generation (AC Transfer Function)

As the ability to internally set a DC voltage with a known amplitude via the Vped was made more difficult in TARGET (version C) (TARGET C) (see 2) , more precise ref, and remember to mention this change and the ability to input a DC voltage externally is prohibited by the AC coupling of the module , remember to introduce ac coupling the decision was made to transition to an AC Transfer Function that uses the expected pulse shape as an input. This approach therefore corrects for the AC effect with the appropriate frequency.

The full dynamic range is once again explored, by injecting pulses of a variety of amplitudes. In order to extract the values that correspond to negative amplitudes in this method, the amplitude of the input undershoot is also monitored. Only the samples that corresponds to the maximum of the input pulse (and minimum of the undershoot) has a "true" amplitude of the input amplitude. Therefore to extract the correct samples, each waveform is fitted with two Landau functions, a fair approximation to the pulse shape (Figure). Consequently, only two samples are extracted per waveform, requiring a much larger population of events ($\tilde{2}$00,000) in order to generate a reliable running average grouped according to $[Module, Channel, StorageCell, InputAmplitude]$. It is important to note that a Transfer Function per storage cell was adopted for TARGET C, as it was found to significantly improve the residuals (see for further discussion).

figure showing the fit

appendix tf investigations

The second step in the generation is identical to the DC Transfer Function. The resulting lookup tables can be seen in Figures & .

add figures

Application

Irrespective of the Transfer Function type, they are stored in a format which enables them to be applied identically. When calibrating a waveform, the relevant lookup table is obtained according to the channel and cell of the sample, and is linearly interpolated to provide the calibrated value in mV.

Performance

Due to its complexity and variety of approaches, the Transfer Function is still one of the most actively discussed aspects of the CHEC calibration, and is most certainly the area where the majority of improvements can be made. Some possibilities for improvement include:

- An improved sample extraction method for the AC Transfer Function Waveform
- Possibilities for a DC approach for TARGET C
- Returning to the approach described in [1] where the pedestal is included inside the Transfer Function
- Alternatives to linear interpolation, such as Piecewise Cubic Hermite Interpolating Polynomial (PCHIP)

- Exchanging the lookup table for a parametrised regression characterisation of the Transfer Function
- Decision between "per storage cell" or "per sampling cell"
- Inclusion of temperature corrections

Appendix provides some insight into the current progression in these active investigations.

tf investigations

Assessing the performance of the Transfer Functions is a more complicated task than for the pedestals. This is largely because instead of a comparison to a null signal, you are instead comparing to an input amplitude which contains its own uncertainty, and could potentially be incorrect. So while the residuals of the Transfer Function may be small, it does not necessarily mean the calibration is accurate. Therefore the most decisive performance indicator should be one that provides an independent measurement on the "correct" amplitude. The most obvious scheme fitting this requirement is the charge resolution, covered in detail by 7. However, while it does hold the drawbacks just mentioned, investigating the residuals through the Root-Mean-Square Error (RMSE) can provide insights on the Transfer Function calibrated unhindered by other components in the detector chain. Figure demonstrates the RMSE for the presently adopted Transfer Functions for TARGET C, compared to a simple calibration with a fixed conversion value $X\ mv/ADC$.

insert figure

obtain sensible value, and talk about the result a bit, non-linearity, show equation for RMSE

For ch7: Remember to talk about how the MC charge resolution provides us insight into performance with perfect Transfer Functions

5.4 Photosensor Calibration

The other primary component in the detector chain that requires calibration is the photosensor itself. As photosensors are a much more common instrument used in a variety of experiments, the calibration procedures typically already exist, and it is a simple case of adapting them to fit our needs.

However, unlike with the TARGET modules, where the procedures are very similar between CHEC-M and CHEC-S, an MAPMT is very different to a SiPMT. Therefore it is logical to deal with the calibration procedure for each of these photosensors separately.

5.4.1 CHEC-M

Photomultiplier tubes have been widely used in Gamma-ray Astronomy since the first Imaging Atmospheric Cherenkov Telescopes (IACTs) , therefore the characterisation of these devices is very well understood. However, MAPMTs are a more recent evolution of the devices, and although they have the same underlying concept, they do suffer from some limitations, such as the inability to tweak the HV on a pixel level, and the electrical crosstalk across the tightly packed pixels .

get source

check checm paper for other limitations

A common method to characterize MAPMTs, and the one we also adopted, is the use of the Single Photo-Electron (SPE) spectrum. The primary result this spectrum provides is the per pixel value to calibrate from the measured signal in mV (or mV*ns for integrated charge) to Photo-Electrons (p.e.). This conversion value is hereafter referred to as the SPE value. In order to investigate this parameter, the photosensor is illuminated with a very low light level (average illumination <1 p.e. per pixel). As the photosensor is essentially a photon counting device, the individual peaks of the photoelectrons that are produced by the photocathode can be identified in the histogram of charge amplitudes. The SPE value is therefore the average charge of the first photoelectron peak. However, the resolution of these peaks can be quite poor, especially for MAPMTs, therefore the resulting distribution is fit with a function that characterises the photosensor:

add equation for mapm spe fit, and reference its origin

SPE fit plots

This SPE value is proportional to the gain of the photomultiplier, and therefore also proportional to the HV applied across the photomultiplier. In order to extract a clear SPE spectrum, the voltage across the MAPMTs are set to the maximum value of 1100 V, thereby maximising the separation between the photoelectron and pedestal peaks.

In order to extrapolate the correct SPE value for other HV settings, the following relation:

Can be used in combination with a logarithmic fit of a dataset where the amplitude is measured as a function of HV to obtain α per pixel.

double check, maybe linear regression in log space?

In order to apply this calibration, the SPE value (with units of $mV * ns * p.e.^{-1}$) per pixel is multiplied by the charge extracted per pixel.

include plot of relation

show a waveform with this factor applied, maybe also the spectrum

plots of the SPE values at different hv sets

5.4.2 CHEC-S

In the transition to SiPMTs, the calibration procedure for the photosensors was revised to better utilise the upgraded functionality of CHEC-S.

Gain Matching

Firstly, the voltage across the photosensors are now configurable per superpixel (group of 4 pixels) as opposed to per module. This allows the voltage to be fine-tuned to produce an identical gain response on a per superpixel level.

mention superpixels in ch3

The procedure for this is illustrated in Figure :

gain matching figure

- The camera is illuminated with approximately 50 p.e.
- The waveforms are readout and averaged per superpixel (excluding any dead pixels)
- The next voltage settings are calculated such that they will reduce the spread in the pulse height of the averaged waveforms
- The new voltage setting are applied, and the process is repeated

This iterating approach reduces the gain spread between pixels from (Figure)

values

add final comparison figure

need a note here or in ch2 about how other parameters of an sipmt change with hv

The additional benefit of this calibration is that changes in temperature, which would normally affect the gain, can be accounted for by changing the HV, therefore maintaining a constant gain response across the camera. This particular in situ calibration has not yet been implemented, but is intended for the future.

plot with gain vs temperature?

SPE Calibration

The second step in the CHEC-S photosensor calibration differs according to the purpose of the dataset being calibrated. In order to completely characterise the camera, and produce the Charge Resolution results, the per pixel SPE value must be obtained, and used to produce the absolute charge in a waveform (the complete Charge Resolution procedure can be found in Chapter **??**).

The function that characterises the SPE distribution of an SiPMT is not wildly different to that of an MAPMT, but does include the significant contribution of the optical crosstalk:

write function

The other significant difference in the SPE distribution of an SiPMT is the improved resolution of the peaks. Typically when an SiPMT is illuminated at , peaks from can be identified. Figure shows the SPE spectrum for the model of SiPMT we have installed into the camera. However, due to the inclusion of the other electronics in the camera, this incredible resolution is mostly suppressed, but is still significantly better than what was observed with CHEC-M.

illumination

range of peaks

obtain spe figure of sipm on

reference chec-m figure

Figure shows the SPE spectrum and fit for a pixel in our camera. The resulting parameters are

insert figure

talk about the spe fit parameters, and show some histograms

Flat-Fielding

Alternatively, in the default data-taking mode of on-sky Cherenkov images, the flat-fielding approach is used. This exists as a software extension to the gain-matching to further unify the response across the camera. With an illumination of approximately 50 p.e. (as with the gain matching), the coefficients are extracted such that the charge measured in each pixel is the same (after accounting for the difference in illumination between pixels due to the beam profile and curved geometry of the focal plane). These coefficients differ in those obtained via the SPE method as they include the relative Photon Detection Efficiency (PDE) between pixels in the correction.

The argument between flat-fielding according to gain response (SPE fitting) or according to illumination response (method we are adopting) is a common one among IACTs , and is also a current topic among the different CTA telescopes. The reason we have chosen to adopt the latter is it reduces the pixel-to-pixel variations in their response to being illuminated, which is important for Cherenkov shower images. The measured charge in each pixel will not be exactly representative of the number of photoelectrons, but instead it will be representative of the number of photons. However, in order to keep the charge extracted in relatable units, a single nominal $mV * ns * p.e.^{-1}$ conversion value will be applied to the entire camera.

find references where HESS/-MAGIC differ in their approach

needs some demonstration of its impact, some plots for example, that continue on from the gain matching plots

5.5 Other

In addition to the calibrations mentioned thus far, there are a few less important calibrations that could improve the performance further.

5.5.1 Timing Corrections

Due to the routing of the electronics in the front-end, the electrical signal path is slightly different per channel, causing a small difference in apparent arrival of the pulse in the waveform. The relative arrival time per pixel can be seen in Figure .

add camera image showing relative time

Not only does this need to be taken into consideration when investigating the timing performance, it also can have a significant impact on the charge extraction, which typically relies on other pixels (neighbouring or entire camera, see Chapter 6) sharing an compatible pulse time. The effect of a 1 ns incorrectly extracted charge (when the peak finding is done using the waveforms from all pixels) can have the impact on the charge resolution shown in Figure

show impact of an incorrect time extraction on charge resolution, maybe of just TM?

The first approach in correcting for this affect is to shift the charge extraction by the timing correction. However, current charge extraction methods do not operate on time scales smaller than the waveform binning, therefore approaches on how to adapt those methods for corrections below that scale are being discussed.

5.5.2 Temperature Corrections

Temperature is most likely the most prominent factor in changing the calibration values on short scales, and has been mentioned in almost every approach. Investigations into exactly how these parameters change with temperature are ongoing, but examples can be seen in:

- Figure

  Pedestal ramp

- Figure

  TF Variation with temp

- Figure

  Gain variation with temp

In the future we intend to have a calibration pipeline that is independent of these temperature effects. For the photosensors this is very simple, as the voltage across them can be altered to account for the temperature changes. For the TARGET modules, this may require an additional lookup table, or an extra dimension to the existing tables.

5.5.3 LED Flashers

Although not technically a part of the waveform processing chain, the LED flashers have an important role in the calibration pipeline, especially for the final operation of the CHEC cameras in CTA. Their purpose is to allow us to perform in situ calibration, by uniformly illuminating the camera via reflection in the secondary mirror. However to achieve this, we must characterize and calibrate the LEDs such that we accurately know the illumination they are providing.

include some results on the LED calibration, and also mention their temperature dependence.

5.6 Future

During the long development of CHEC, the calibration procedure has evolved a lot, and multiple iterations have occurred to either:

- accommodate the changes required in the upgrades of hardware (such as from TARGET (version 5) (TARGET 5) to TARGET C)
- simplify the calibration to save on resources
- or account for additional factors, thereby improving the calibration (such as the AC contribution to the Transfer Functions)

Therefore, while each iteration improves in one aspect, it may be at the expense of the others. As a result, the TARGET calibration procedure described in this chapter appears quite complicated compared to the approaches detailed in [2] and [1]. The primary next step in the calibration development for CHEC is therefore to review the procedure used, with the aim to produce an approach that is simpler, includes aspects such as temperature dependence, and meets the requirements and processing rates required by CTA.

6

Pipeline Reduction

Contents

5.1 Plan **8**
5.1.1 Topics 8
5.1.2 Questions 8
5.2 Introduction **8**
5.3 TARGET Calibration **9**
5.3.1 Electronic Pedestal Subtraction 9
5.3.2 Transfer Function 11
5.4 Photosensor Calibration **14**
5.4.1 CHEC-M 14
5.4.2 CHEC-S 15
5.5 Other **17**
5.5.1 Timing Corrections 17
5.5.2 Temperature Corrections 18
5.5.3 LED Flashers 18
5.6 Future **19**

:

6.1 Plan

6.1.1 Topics

- Charge Extraction Methods
- Image cleaning
- Shower reconstruction
  - Hillas
  - Impact
  - model
  - Neural Nets
  - ++
- Energy Reconstruction
- Direction Reconstruction

6.1.2 Questions

- ?

7
Camera Performance

Contents

6.1 Plan **20**
6.1.1 Topics 20
6.1.2 Questions 20

:

7.1 Plan

7.1.1 Topics

- Charge Resolution
- TF Investigations
- Different NSB
- MC Validation
- MC Performance

7.1.2 Questions

- What other criteria?
  - Trigger performance - even though I haven't contributed

8

On-Sky Pipeline

Contents

7.1 Plan **21**
7.1.1 Topics 21
7.1.2 Questions 21

:

8.1 Plan

8.1.1 Topics

- Decided upon reduction methods
- Potentially different than for performance chapter
- CHEC-M campaign
- MC CHEC-S
- Future observations
- Jupiter observations (Beyond cherenkov?)

8.1.2 Questions

- ?

9
Summary

Contents

8.1 Plan **22**
8.1.1 Topics 22
8.1.2 Questions 22

References

[1] A. Albert et al. “TARGET 5: A new multi-channel digitizer with triggering capabilities for gamma-ray atmospheric Cherenkov telescopes”. In: *Astroparticle Physics* 92 (2017), pp. 49–61. arXiv: 1607.02443. URL: http://linkinghub.elsevier.com/retrieve/pii/S0927650517301524.

[2] K. Bechtol et al. “TARGET: A multi-channel digitizer chip for very-high-energy gamma-ray telescopes”. In: *Astroparticle Physics* 36.1 (2012), pp. 156–165. arXiv: 1105.1832. URL: http://dx.doi.org/10.1016/j.astropartphys.2012.05.016.